ACS NANO
Cite This: ACS Nano 2018, 12, 198−207
www.acsnano.org
ARTICLE

Going Vertical To Improve the Accuracy of Atomic Force Microscopy Based Single-Molecule Force Spectroscopy

Robert Walder,[†] William J. Van Patten,[†] Ayush Adhikari,[†] and Thomas T. Perkins*[,†,‡]

[†]JILA, National Institute of Standards and Technology, and University of Colorado, Boulder, Colorado 80309, United States
[‡]Department of Molecular, Cellular, and Developmental Biology, University of Colorado, Boulder, Colorado 80309, United States

Supporting Information

ABSTRACT: Single-molecule force spectroscopy (SMFS) is a powerful technique to characterize the energy landscape of individual proteins, the mechanical properties of nucleic acids, and the strength of receptor−ligand interactions. Atomic force microscopy (AFM)-based SMFS benefits from ongoing progress in improving the precision and stability of cantilevers and the AFM itself. Underappreciated is that the accuracy of such AFM studies remains hindered by inadvertently stretching molecules at an angle while measuring only the vertical component of the force and extension, degrading both measurements. This inaccuracy is particularly problematic in AFM studies using double-stranded DNA and RNA due to their large persistence length ($p \approx 50$ nm), often limiting such studies to other SMFS platforms (*e.g.*, custom-built optical and magnetic tweezers). Here, we developed an automated algorithm that aligns the AFM tip above the DNA's attachment point to a coverslip. Importantly, this algorithm was performed at low force (10−20 pN) and relatively fast (15−25 s), preserving the connection between the tip and the target molecule. Our data revealed large uncorrected lateral offsets for 100 and 650 nm DNA molecules [24 ± 18 nm (mean ± standard deviation) and 180 ± 110 nm, respectively]. Correcting this offset yielded a 3-fold improvement in accuracy and precision when characterizing DNA's overstretching transition. We also demonstrated high throughput by acquiring 88 geometrically corrected force-extension curves of a single individual 100 nm DNA molecule in ∼40 min and versatility by aligning polyprotein- and PEG-based protein−ligand assays. Importantly, our software-based algorithm was implemented on a commercial AFM, so it can be broadly adopted. More generally, this work illustrates how to enhance AFM-based SMFS by developing more sophisticated data-acquisition protocols.

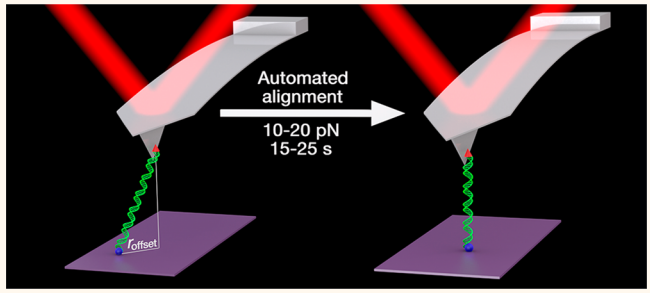

KEYWORDS: *atomic force microscopy, DNA overstretching, protein folding, polyprotein, single-molecule force spectroscopy*

Over two decades ago, atomic force microscopy (AFM)-based single-molecule force spectroscopy (SMFS) emerged as a powerful tool to measure the dynamics and energetics of individual proteins[1] and protein−ligand interactions.[2,3] Notwithstanding several early successes in studying DNA at high force by AFM,[4,5] optical traps and magnetic tweezers rapidly emerged as the SMFS modality of choice for studying mechanical properties of DNA, RNA, and, more generally, protein−nucleic acid interactions.[6−8] Historically, this bifurcation in biomolecular systems studied by AFM arose from two well-documented issues: (i) the comparatively poor force precision and stability of AFM and (ii) the widespread use of nonspecific attachment schemes in AFM-based assays.[7,8]

Sub-piconewton sensitivity and stability on a commercial AFM can now be routinely achieved by eliminating[9] or spatially patterning[10] the gold coating of the AFM cantilever, enabling equilibrium studies of membrane-protein folding by AFM.[11] Efficient site-specific attachment of DNA to AFM tips and coverslips facilitates repeated stretching of the same individual DNA molecule tens to hundreds of times, improving throughput.[12] Thus, the field of nucleic acid force spectroscopy is poised to leverage two significant advantages of AFM. First, modern commercial AFMs are user-accessible, particularly compared to custom-built optical traps. Second, AFMs can accommodate significantly shorter, and therefore stiffer, linkers relative to optical traps, improving spatiotemporal resolution.[13] Yet, one key issue remains: force accuracy. Accuracy is degraded because double-stranded nucleic acids are stiff, with a persistence length (p) of ∼50 nm,[14] and therefore adopt

Received: August 11, 2017
Accepted: December 15, 2017
Published: December 15, 2017

DOI: 10.1021/acsnano.7b05721
ACS Nano 2018, 12, 198−207

extended conformations in comparison to polyethylene glycol (PEG) or unfolded protein (both of which have $p \approx 0.4$ nm).[1,15] This extended conformation, in turn, leads to the DNA's anchor point to the coverslip not being positioned directly under its attachment point to the AFM tip (r_{offset}). As a result, the DNA is stretched at an unknown angle while measuring only the vertical component of the applied force (Figure 1a). Indeed, more than a decade ago, theoretical work predicted significant errors in the absolute force applied to the DNA when pulling at an angle.[16] More recently, concerns with pulling geometry have been extended beyond stiff polymers to include flexible linkers[17] commonly used in protein−protein and protein−ligand studies.[18]

Pioneering experimental work by Ke *et al.* investigated the accuracy of DNA studies *via* AFM and showed that pulling at an angle compromises both force and extension measurements.[19] Such results confirmed earlier theoretical concerns[16] and have been verified by subsequent work.[20] To illustrate this problem, we show a force-extension curve for a DNA molecule pulled vertically and at an angle (Figure 1b, blue *versus* red, respectively). As expected, the molecule pulled at an angle appeared to undergo DNA's well-studied overstretching transition[21,22] at a force considerably below the canonical 65 pN because only the vertical component (F_z) of the total force (F) applied was measured, recapitulating a similar reduction seen in earlier work when stretching a polymer of pyranose at an angle.[23] Interestingly, for stiff polymers like DNA, the extension measurement is corrupted beyond a simple geometric misalignment resulting from a substantial r_{offset}. This complexity arises because the attachment point to the tip is more likely to occur a substantial distance up from the apex of the tip (z_{offset}), an error that is convolved with the r_{offset} between the attachment points when trying to determine DNA extension (Figure 1a).

In an important first step toward a general solution to this problem, Kuhner *et al.* scanned the tip in a series of squares of increasing size at constant height over the surface when studying a flexible polymer.[23] Rivera *et al.* then adapted an orbital-based scanning scheme to determine the direction to the anchor point while stretching DNA by developing a software-based algorithm coupled with custom hardware integrated into a commercial AFM.[24] However, these two implementations led to either a peak force of >300 pN[23] or a relatively high force (~80 pN) over long periods (~80 s).[24] Such force profiles often lead to the rupture in one of the linkages connecting the tip to the surface through the biomolecule of interest and is particularly problematic for the site-specific coupling ubiquitously used in DNA studies (*i.e.*, streptavidin−biotin and antidigoxigenin−digoxigenin)[6−8] since these bonds may only last only a few seconds to tens of seconds at 80 pN.

Here, we developed and implemented an automated algorithm on a commercial AFM that aligns a target molecule's attachment point to the tip above its attachment point to a coverslip. Our constant-force algorithm avoided applying a high peak force during initial direction finding and accelerated the subsequent alignment. As a result, our method was relatively fast (15−25 s) and performed at low force (10−20 pN). This improved throughput, allowing us to experimentally measure r_{offset} and its distribution. As expected, the average value was substantial for 100 nm DNA (24 ± 18 nm; mean ± standard devidation (SD), $N = 321$) and 650 nm DNA (180 ± 110 nm, $N = 174$). From the same data set, we also determined the z_{offset} and its distribution, which yielded similar values of 26 ± 13 and

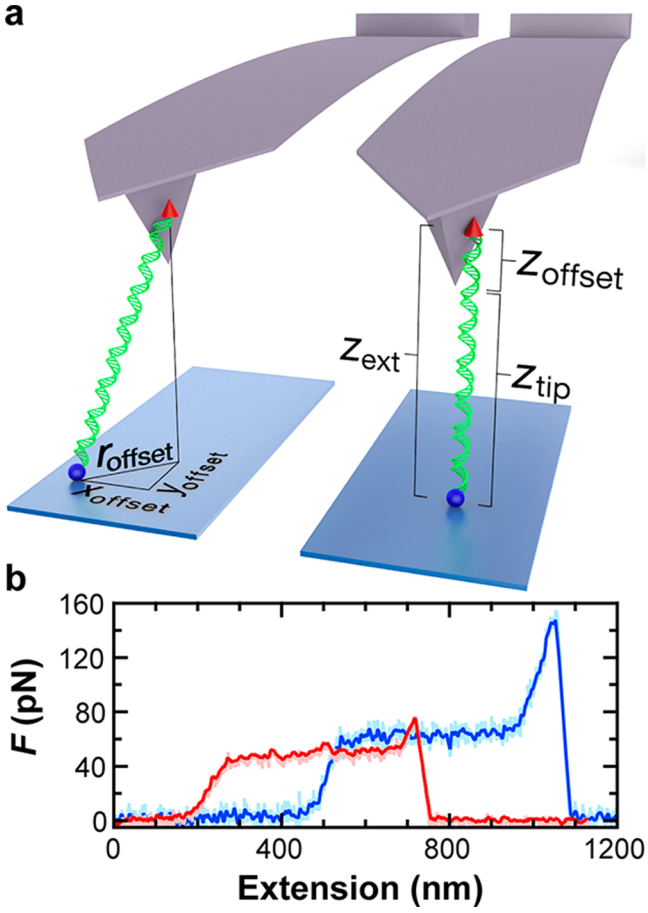

Figure 1. Improving the accuracy of AFM-based SMFS. (a) Cartoon defining the geometry of stretching DNA before and after alignment when using site-specific attachment chemistry (red pyramid, blue sphere). Since double-stranded DNA is a stiff polymer, an unaligned assay experiences significant lateral offset (r_{offset}), in addition to a vertical offset (z_{offset}) arising from the DNA attaching to the cantilever at a point vertically displaced from the tip apex. For clarity, only one instance of each of the surface chemistry moieties is shown. However, the AFM tip is densely coated. Hence, it is common for the DNA to bind vertically displaced from the tip apex, as illustrated. The surface density of the DNA was chosen to promote stretching a single molecule as opposed to multiple in parallel. (b) Force-extension curves in an aligned (blue) and an unaligned (red) geometry with different z_{offset}. Importantly, the aligned curve shows DNA overstretching at the correct force (~65 pN) while the unaligned curve does not.

230 ± 120 nm, respectively. Vertically aligning a DNA-based AFM assay yielded a 3-fold improvement in the accuracy and precision when using DNA's overstretching transition[21,22] as a force standard.[25] We also demonstrated high throughput by acquiring 88 geometrically corrected force-extension curves of a single individual 100 nm DNA molecule in ~40 min. Finally, given recent concerns with geometry-induced errors in AFM-based SMFS with flexible linkers,[17] we also demonstrated rapid (8−10 s) geometric correction of a short polyprotein ($L = 92$ nm) and protein−ligand PEG-based (MW = 10 kDa) assay. Therefore, a diverse range of widely used AFM-based assays can immediately benefit from improvements in precision and accuracy by implementing a vertical stretching geometry.

Given our goal to improve the accuracy of AFM-based SMFS, we used target molecules (DNA or protein) site-specifically attached to a coverslip and an AFM tip.[12] A key

DOI: 10.1021/acsnano.7b05721
ACS Nano 2018, 12, 198−207

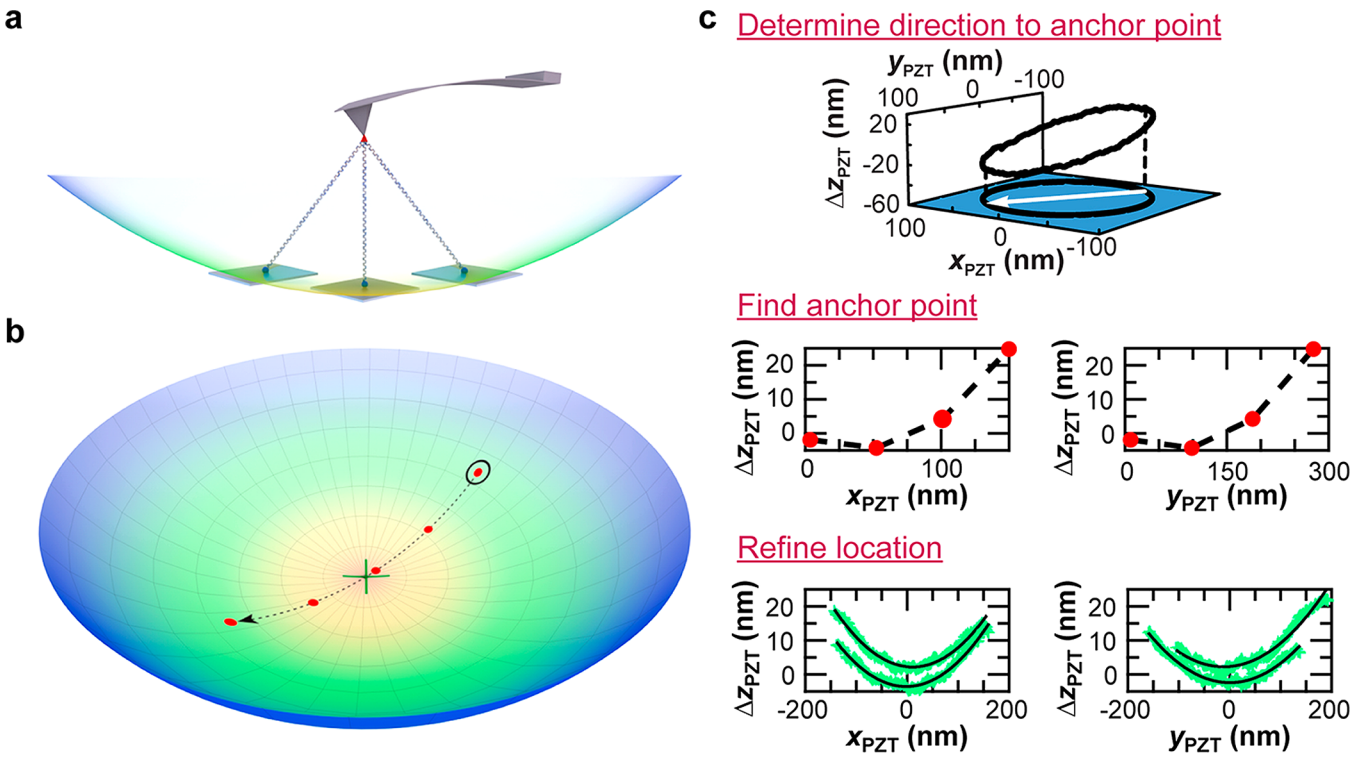

Figure 2. Three-step algorithm for efficient alignment. (a) Illustration of the parabolic motion of the z-position of the PZT stage (z_{PZT}) when stretching DNA under constant measured force (F_z) at different lateral displacements. Vertical pulling geometry is achieved at the minimum point of this parabola. (b) Illustration of two-dimensional (2D) alignment under constant force shows z_{PZT} mapping out a 2D parabolic-like surface. The three steps of the alignment algorithm are projected onto this surface: an initial orbital scan (black circle), motion toward the approximate anchor point (red dots), and a refinement in anchor point location (green cross). (c) Quantifying the steps of the alignment process. (Top panel) To determine the direction toward the surface anchor point, the change in z_{PZT} (Δz_{PZT}) under constant force is recorded as the stage executes lateral circular motion. The direction of the arrow is determined from the peak and the minimum in Δz_{PZT} and points toward the anchor point. (Middle panel) To find the approximate location of the anchor point (*i.e.*, the minimum in Δz_{PZT} while stretching the DNA under constant force), Δz_{PZT} was measured during a series of discrete steps along the direction determined by the orbital scan. Note that the step size along the x- and y-axes varies depending on the angle of motion relative to these measurement axes. Dashed line to guide the eye. (Bottom panel) To refine the location of the anchor point, Δz_{PZT} was sequentially measured along each coordinate axis, and the resulting data were fit to a parabola with the location of the minimum used as the updated estimate for the anchor point along each axis. This final 2D refinement process was usually repeated 2−3 times.

feature of this recently developed assay is the target molecule was covalently coupled to a PEG-coated surface while being attached to a PEG-coated tip *via* a streptavidin−biotin linkage. Covalently coupling ensures that the target molecule remained on the surface after rupture from the tip so it could be subsequently remeasured. The PEG coating on both the tip and the coverslip suppressed nonspecific adhesion that would otherwise obscure unfolding transitions of more dynamic biomolecules such as ribozymes[26] and DNA hairpins[27] that occur at low force by traditional AFM standards (10−15 pN).[7,8]

RESULTS AND DISCUSSION

Rapid Algorithm for Vertical Alignment. We developed a three-step algorithm for aligning a target molecule's surface anchor point directly below its attachment point to the tip (Figure 2). The two critical design requirements for our algorithm were minimizing the applied force during alignment process and achieving a rapid alignment. The key insight was to perform the vertical alignment at constant force. We illustrate this concept with a one-dimensional (1D) sketch (Figure 2a), which shows that lateral offsets away from vertical alignment under constant measured force (F_z) were compensated for by raising the vertical stage position (z_{PZT}). Hence, vertical alignment under constant F_z was transformed into a task of finding the lowest z_{PZT} in two dimensions (2D) (Figure 2b). The three steps in our algorithm were (i) determining the direction to the anchor point, (ii) finding the anchor point, and (iii) refining its location (Figure 2c). All stage motion was done under closed-loop control. For succinctness, we illustrate the algorithm by providing user-specified settings for 650 nm DNA. Table S1 (Supporting Information) provides these values for all of the constructs studied, and Figure S1 provides a flowchart illustrating the logic of vertical-alignment algorithm embedded within a higher-level data-acquisition scheme.

To initiate an individual experiment, we brought the tip into contact with the surface for 2 s at a relatively low force (100 pN), approximately 10-fold less than the force used to promote nonspecific adhesion.[28] We then retracted the tip at a constant velocity (v = 1 μm/s). Our vertical-alignment algorithm was then triggered after detecting a good candidate molecule. To do so, we programmed the AFM controller to monitor the measured force in real time and automatically stop retraction when F > 20 pN at an extension (x_{DNA}) greater than ∼20% of the target molecule's contour length. This criterion suppressed false positives arising from nonspecific adhesion between the tip and the surface at low extension. Importantly, to improve force control, we programmed our AFM controller to respond

DOI: 10.1021/acsnano.7b05721
ACS Nano 2018, 12, 198−207

to the average force (smoothed to 1 kHz) rather than high-bandwidth data (50 kHz). Subsequent data during aligned force-extension curves were recorded at 50 kHz or 5 MHz, depending on the application.

Upon detection of successful attachment, the algorithm's first step was to determine the direction to the anchor point using an orbital-based method, akin to Rivera *et al.*'s earlier work.[19] In particular, after activating a force clamp, we recorded z_{PZT} while moving the stage at a constant velocity in a small circle, where the radius of the circle varied with the contour length of the target molecule (*e.g.*, 75 nm for a 650 nm DNA) (Figure 2c, top panel). We next determined the approximate direction toward the anchor point by analyzing z_{PZT}. The needed direction pointed from the maximum in z_{PZT} to the minimum in z_{PZT}. For simplicity of presentation, we plot Δz_{PZT} rather than its absolute value.

To find the location of the anchor point, we moved the stage along the determined direction in a series of fixed-size steps (*e.g.*, 150 nm for 650 nm DNA) while averaging z_{PZT} over 250 ms of data under constant F (Figure 2c, middle panel). This section of the algorithm stopped once z_{PZT} increased. We then moved to the lateral location (x_{PZT}, y_{PZT}) associated with the lowest recorded z_{PZT}.

The third step of the algorithm moved the stage at constant velocity for a fixed distance (150 nm for 650 nm DNA) in each direction along the x- and y-axes, while z_{PZT} was measured under constant F. We set the range of this motion (*e.g.*, 150 nm) to generate a parabolic-shaped trace of z_{PZT} *versus* lateral motion (Figure 2c, lower panel), which then allowed a simple fit to this trace to determine the minimum point in z_{PZT} along each coordinate axis. Note, when there is no clear minimum (see Figure 6b, green trace), the algorithm used the lateral position at the minimum value for z_{PZT}. Finally, we moved the stage to that lateral location. This refinement procedure was then repeated multiple times (typically 2−3) until two subsequent anchor point locations agreed to within a user-defined precision (*e.g.*, 7 nm for 650 nm DNA). We then lowered the tip into gentle contact with the surface (F = 100 pN), which provides a revised determination of the surface height after alignment. The assay was now aligned with high precision for subsequent force spectroscopy studies ($\Delta\theta \approx 7/650$).

Although the run time for individual molecules varied, our algorithm typically took 15−25 s to execute for 100 nm DNA and was quicker for polyproteins (8−10 s). Hence, the algorithm was relatively fast in comparison to prior work (80 s).[24] When using DNA containing a single terminal biotin, this combination of speed with low applied F allowed a high percentage (94%; N = 94) of initial attachments to become vertically aligned with the tip (*i.e.*, without a rupture between the DNA and the tip). The two primary limitations on the execution time of our algorithm were (i) averaging the Brownian motion of the cantilever and (ii) communication between the AFM controller (ARC2, Asylum Research) and the PC-based software controlling the AFM (Igor Pro, WaveMetrics). We chose parameters for each step of the algorithm that balanced the need for execution speed while ensuring a precise signal for determining the vertical pulling position. We note that the parameters used in these experiments (Table S1) were determined when measuring with a long, soft cantilever [L = 100 μm; k = 8 pN/nm (Olympus)] that had its gold coating removed for improved force stability.[9] For cantilevers with lower noise and better

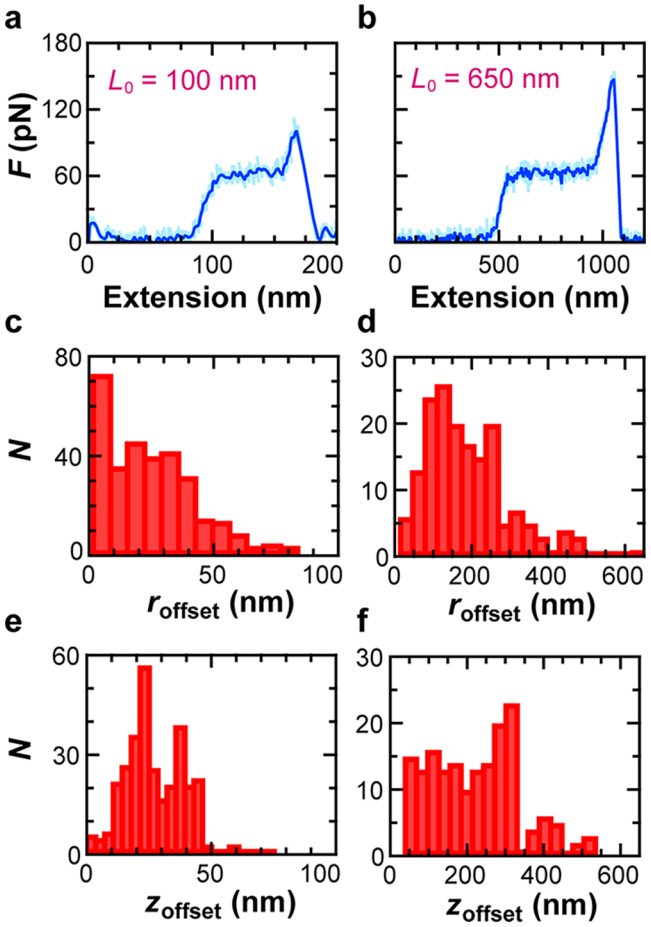

Figure 3. Characterization of geometric errors when pulling on DNA. (a,b) Force-extension curves acquired after alignment for 100 and 650 nm long DNA, respectively. (c,d) Distribution in lateral offset (r_{offset}) for 100 and 650 nm DNA determined from 321 and 174 DNA molecules that were geometrically aligned, respectively. (e,f) Distribution in vertical offset (z_{offset}) for 100 and 650 nm DNA determined from the same set of data.

temporal resolution[10,29,30] or higher-strength mechanical linkages to the tip,[31,32] we anticipate quicker algorithm execution without compromising alignment precision.

Importantly, our software-only alignment scheme was implemented on a commercial AFM (Cypher ES, Asylum Research). Hence, it can be immediately implemented at no cost on Asylum Research AFMs or custom-built AFMs controlled by an Asylum controller.[33−35] To promote such adoption, we have shared the source code for our algorithm and accompanying documentation *via* GitHub.[36] Our algorithm is extendable to other commercial AFMs that support adequate flexibility in creating user-defined data-acquisition protocols.

Characterizing the Uncorrected Geometry of an AFM-based DNA Assay. Prior studies have not experimentally documented the distribution in misalignments when stretching DNA by AFM (*i.e.*, r_{offset}, z_{offset}). To address this issue, we first measured a set of force-extension curves for two different length DNAs (100 and 650 nm) (Figure 3a,b) by probing the surface in a grid-based raster scan (Figure S1). We next deduced r_{offset} by computing the difference in lateral stage position before and after alignment (Figure 3c,d). To deduce z_{offset}, we initially fit each aligned force-extension curve to an extensible worm-like chain model,[37] which yielded an apparent

DOI: 10.1021/acsnano.7b05721
ACS Nano 2018, 12, 198−207

contour length L_0^{app}. We then calculated the vertical offset using $z_{offset} = L_0 - L_0^{app}$ (Figure 3e,f). Such characterization required our site-specific coupling to ensure that the target molecule was stretched across its full contour length, independent of where it attached to the tip. To confirm this assumption, we analyzed force-extension curves that exhibited the complete overstretching of DNA. The resulting analysis showed that width of the overstretching plateau was the expected 70% of target molecules contour length,[21,22] regardless of z_{offset} (Figure S2). To facilitate this characterization, we used a more mechanically robust coupling to the streptavidin-coated tip by using a DNA molecule terminally labeled with four biotins spaced once every helical turn *via* a PCR primer.

Our analysis showed the lateral offsets were substantial and broadly distributed. In particular, for 100 nm DNA molecules, r_{offset} ranged from 1 to 80 nm and an average value of 24 ± 18 nm (mean ± SD; N = 321) (Figure 3c). We observed a similar broad distribution for 650 nm DNA molecules with a range from 7−631 nm and an average value of 180 ± 110 nm (mean ± SD; N = 174). In other words, we determined that the average lateral offset for both DNA lengths was approximately $1/4L_0$.

Interestingly, the vertical offset was similar in size or even slightly larger than the lateral offset. Specifically, z_{offset} ranged from 2 to 74 nm for 100 nm DNA with an average value of average z_{offset} of 26 ± 13 nm (mean ± SD) (Figure 3e). For 650 nm DNA, we measured a range of 31−527 nm for with an average value of 230 ± 120 nm (mean ± SD) (Figure 3f). In retrospect, such large vertical offsets could have been anticipated given that the streptavidin coating of the cantilever is not restricted to the tip apex but densely deposited over the entire cantilever. Specifically, the number of streptavidin molecules increases at a given vertical displacement away from the tip apex due to increasing surface area. Hence, there are an increasing number of binding sites, which favors attaching with a larger vertical displacement from the tip apex. This bias, coupled with a stiff polymer, then leads to a substantial average z_{offset}.

Improving the Precision and Accuracy of DNA Studies. To characterize the degree of improvement resulting from vertically aligning an AFM-based DNA assay, we quantified DNA's overstretching transition,[21,22] a force standard for SMFS assays.[25] The overstretching force (F_{OST}), here defined as the force value at the midpoint in the force plateau (Figure 4, inset), is highly reproducible and varies minimally with ionic conditions,[38] temperature,[39,40] and stretching rate.[5] Nonetheless, we used the same ionic conditions, temperature, and force definition as a recent optical-trapping result that is used here as the reference value F_{OST}^{REF} = 65.0 ± 0.5 pN (mean ± standard error of the mean; N = 22) (Figure 5, green dashed line).[41] Specifically, we stretched 84 100 nm DNA molecules in a standard AFM assay and 93 ones after alignment (Figure S3). Unaligned records yielded F_{OST} = 58.5 ± 5.0 pN (mean ± SD) *versus* F_{OST} = 67.0 ± 1.8 pN for aligned ones (Figure 4, red and blue, respectively). Force precision was determined from the standard deviation in the distribution, whereas force accuracy was determined from $\Delta F/F_{OST}^{REF}$, where ΔF is the difference between the measured mean of F_{OST} reported here and F_{OST}^{REF}. Hence, vertical alignment yielded a ∼3-fold improvement in both the precision and accuracy of determining F_{OST} when comparing unaligned *versus* aligned assay. Interestingly, the aligned assay now had a force accuracy of 3% and was therefore likely limited by the precision in calibrating cantilever stiffness,

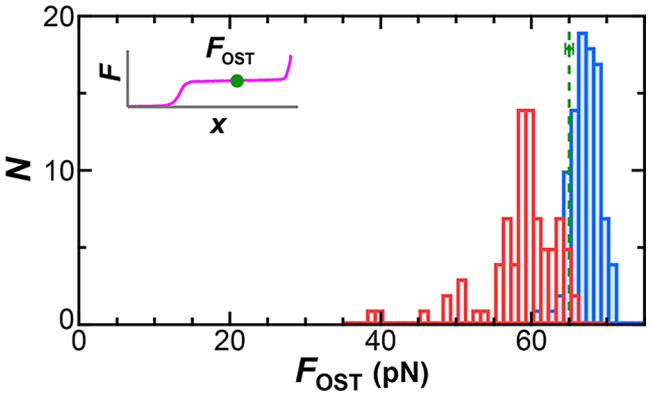

Figure 4. Histograms comparing the overstretching transition force (F_{OST}) of 100 nm DNA with and without vertical alignment (blue *versus* red, respectively). More quantitatively, aligned records yielded F_{OST} = 67.0 ± 1.8 pN (mean ± SD; N = 93) while the unaligned ones gave 58.5 ± 5.0 pN (mean ± SD; N = 84). Under the same ionic conditions and temperature, recent optical-trapping results yielded F_{OST} = 65.0 ± 0.5 pN [mean ± SD; N = 22 (green diamond and dashed line)], where the error bars represent the uncertainty in the measurement.[41] Hence, vertical alignment led to a ∼3-fold improvement of both the precision and accuracy of AFM-based SMFS studies of DNA stretching. (Inset) Canonical force-extension curve illustrating the definition of F_{OST} as the force value midway through the overstretching transition.

which is reported to be 3% when comparing the same individual cantilever among leading laboratories.[42] Looking forward, the improved precision and accuracy of vertically aligned assay offers a means to benchmark future advances in cantilever calibration schemes and verify calibrations of individual cantilevers, particularly when using cantilevers with modified geometries to enhance force precision and stability.[43]

High-Throughput, Geometrically Corrected Stretching of 100 nm DNA. To demonstrate increased accuracy coupled with relatively high throughput, we repeatedly measured the same individual 100 nm DNA in a fully automated fashion by embedding our vertical-alignment algorithm (Figure 2) within a higher-level data-acquisition protocol (Figure S1). Specifically, after rupture of the streptavidin−biotin bond linking the DNA to the tip, we brought the tip back down into gentle contact with the surface to promote reattachment as the assay was vertically aligned. If successful attachment was detected based on the above criteria (*e.g.*, F > 20 pN at x_{DNA} > 20 nm), the data-acquisition protocol would trigger the vertical-alignment algorithm and then record a force-extension curve at constant velocity (v = 1 μm/s). We note that it was important to run the vertical-alignment algorithm for each individual attachment because DNA's extended conformation leads to reattachment at a different location on the tip, both horizontally and vertically. After 10 unsuccessful attachment attempts, the stage was raster scanned laterally to search for another molecule.

To illustrate this improved throughput, we measured 88 vertically aligned force-extension curves in ∼40 min from a single individual DNA molecule (Figure 5). Importantly, this time incorporates all the required functions, including acquiring the initial force-extension measurement to determine if a molecule was attached, executing the vertical-alignment algorithm, measuring the aligned force-extension curves, and saving the resulting data. As in Figure 4, the accuracy of the data was improved with each force-extension curve showing the

DOI: 10.1021/acsnano.7b05721
ACS Nano 2018, 12, 198−207

overstretching transition at ~65 pN, a result that also confirmed a single molecule was studied. In contrast, when we relied upon nonspecific adhesion, only 0.6% of attempts yielded such high-quality force-extension curves, defined as those containing only a single rupture.[12] Moreover, these unaligned force-extension curves typically did not show overstretching at the canonical force of 65 pN (Figure 1a and Figure 4). Thus, it is noteworthy that we can now acquire vertically aligned force-extension curves of DNA more rapidly than unaligned ones acquired with the traditional AFM assay based upon nonspecific adhesion.

The importance of aligning at low force is illustrated by the force-extension curves shown in Figure 5a. For this assay, we used DNA labeled with a single biotin, and a majority of these 88 curves did not exhibit the full DNA overstretching transition (in contrast, see Figure 1a, blue). We attribute this rupture to the failure of the single biotin–streptavidin linkage rather than the mechanically stronger covalent bond coupling the DNA to the coverslip and the streptavidin to the AFM tip. In other words, in the current application, this widely used protein–ligand bond for DNA studies only sustained 65 pN for relatively brief durations. Hence, successful alignment at low force is critical to achieving high throughput.

More broadly, we envision extensions of the present algorithm where a series of individual molecules are probed hundreds to thousands of times, providing enhanced statistical significance coupled with improved accuracy. To do so, further optimization of the higher-level data-acquisition protocol (Figure S1) and the alignment algorithm is required. For instance, the current algorithm failed to reattach to the target molecule due to episodic lateral drift or a rupture during a large lateral movement as seen by examining the positions of the 88 vertically aligned pulls (Figure 5b, dashed line). These and other confounding factors should be amenable to programmatic solutions.

Improving Polyprotein Studies. Polyproteins are the substrate of choice for AFM studies focused on the dynamics and energetics of protein folding.[1,18,44,45] It has long been argued that polyprotein assays, like PEG-based assays, suffer from minimal geometrically induced decrease in force accuracy.[46] In part, this assumption has been based on the lower expected end-to-end distance for a polyprotein, which typically consists of multiple compact, folded domains linked by short flexible polypeptide linkers (p = 0.4 nm).[1] As a result, polyproteins at zero applied force do not adopt the extended conformations sampled by double-stranded nucleic acids (p = 50 nm).

We tested this assumption by using our algorithm to align a polyprotein-based assay (Figure 6a). Given the expected small r_{offset}, we used only the final refinement step of our algorithm, again using multiple iterations (Figure 6b,c). Our substrate was a recently developed short polyprotein[12] containing four domains of NuG2, a fast folding variant of GB1 that has been extensively investigated by AFM.[47,48] To ensure end-to-end stretching of the polyprotein, we used the same site-specific coupling chemistry as in our DNA assay, including a streptavidin–biotin linkage to the AFM tip. Another challenge to aligning a polyprotein is the spontaneous unfolding of domains at elevated force. So, akin to our DNA assay, we initially stretched the polyprotein to an extension that typically unfolded all four domains (Figure 6d, red trace) and triggered execution of alignment algorithm for records beyond that extension that also reached 30 pN. After alignment at a

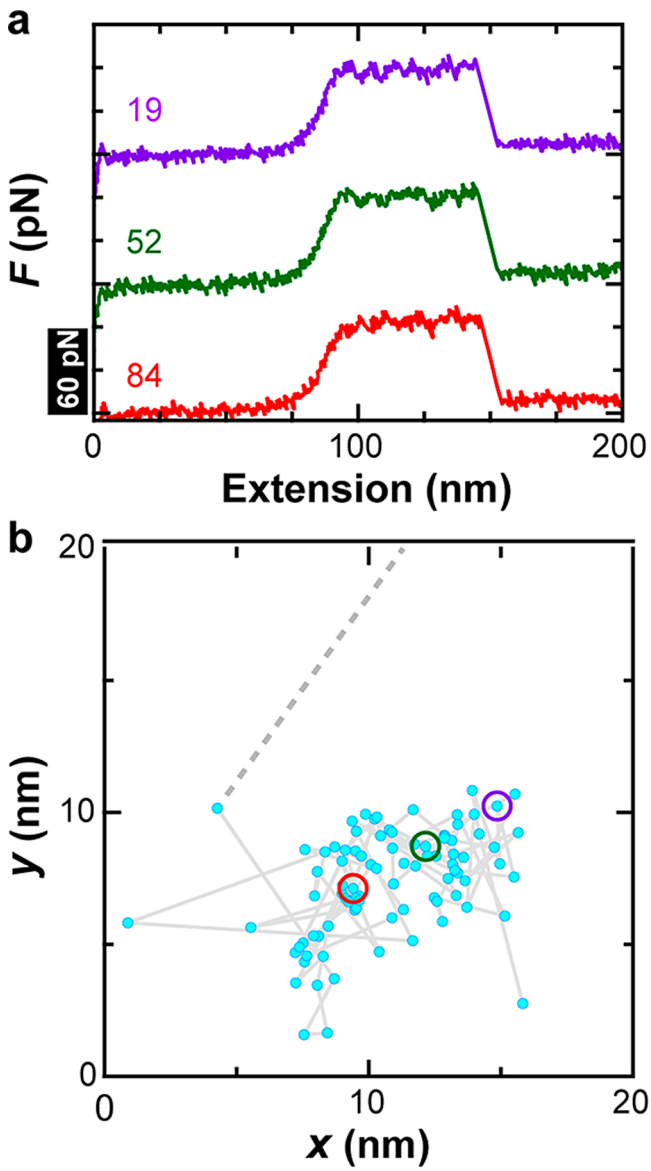

Figure 5. High-throughput, geometric-corrected SMFS data from an individual 100 nm DNA. (a) Three representative force-extension curves from a set of 88 curves acquired during a ~40 min period, where the same individual molecule was repeatedly probed. The number indicates a trace number from this series consisting of 88 such curves. (b) Lateral location of the anchor point as determined by the alignment algorithm. Open circles represent the surface location of the force-extension curves shown in panel a. The final force-extension curve was associated with a large lateral jump in anchor point determination (dashed line).

constant force of 20 pN, the resulting force-extension curve displayed a horizontal shift to longer extensions, and such shifts can be quite substantial [*e.g.*, r_{offset} = 25 nm (Figure 6d, blue trace)]. For completeness, we note though that occasionally our initial stretching did not fully unfold the polyprotein, and the final domain unfolded during the alignment routine. While undesirable, such unfolding was accommodated for by the algorithm *via* several additional cycles of final stage alignment.

Using this algorithm, we then characterized the average r_{offset} for the polyprotein (Figure 6e). While the absolute value was modest [10 ± 8 nm (mean ± SD; N = 73)], it was measurable even for our short polyprotein (L_0 = 92 nm including unfolded

DOI: 10.1021/acsnano.7b05721
ACS Nano 2018, 12, 198–207

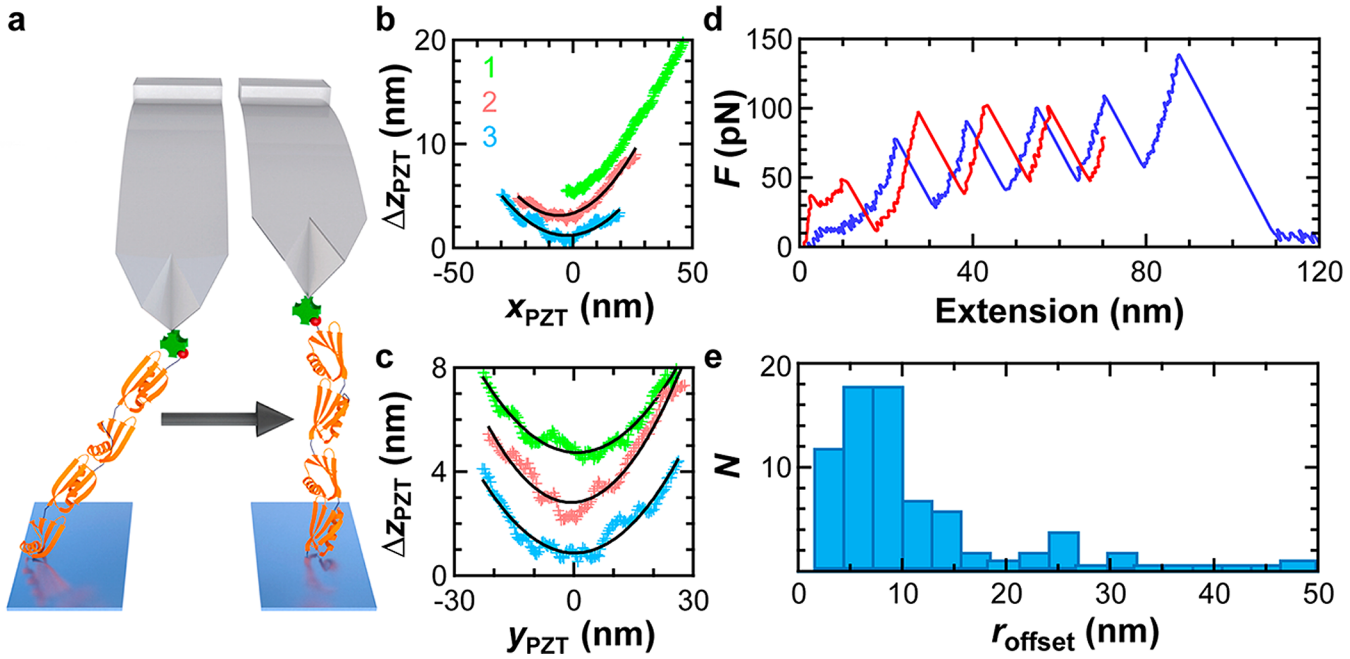

Figure 6. Aligning a polyprotein-based assay for improved accuracy. (a) Illustration of the assay before and after alignment when pulling on a polyprotein consisting of four domains of NuG2, denoted $(NuG2)_4$. Like the DNA assay, the polyprotein was attached to the AFM tip *via* a streptavidin−biotin linkage. (b,c) Change in z_{PZT} (Δz_{PZT}) as a function of lateral motion along each coordinate axis after fully unfolding the polyprotein and executing the alignment algorithm under F = 20 pN. When sufficient curvature was exhibited, the resulting data were fit to a parabola (black lines) to determine the anchor point of the protein. This 2D alignment process was repeated three time along each axis, with each iteration denoted by a separate color. The r_{offset} for this molecule was 25 nm. (d) Force-extension curves before and after alignment for the same individual molecule (red *versus* blue, respectively). Note that the large initial r_{offset} could lead to the misinterpretation of the first domain unfolding as surface adhesion and, hence, this initial force-extension curve as showing only three of the four domains of $(NuG2)_4$ unfolding. (e) Distribution in r_{offset} for $(NuG2)_4$ determined from 73 geometrically aligned molecules.

NuG2 domains, unstructured peptide spacers, and PEG linkers associated with site-specific attachment). Of course, when including the first rupture at low extension in the final analysis, this geometric error is compounded and becomes more significant, even for the average offset of 10 nm [$\theta = \sin^{-1}(r_{offset}/L_0^1) = 22°$)] where L_0^1 is the contour length prior to the unfolding of the first domain (~27 nm in Figure 6d). Lateral offsets larger than the mean r_{offset} will lead to a larger angular misalignment. This simple calculation is perhaps even more relevant when embedding a target protein within a larger polyprotein construct, particularly when the target protein is the first domain to unfold.[12] In such an assay, all of the target protein's unfolding events are subject to a reduction in force accuracy due to angular misalignment. Hence, looking forward, improved force accuracy afforded by the alignment algorithm presented here is expected to improve AFM-based SMFS studies of not only nucleic acids but also proteins and protein−ligand interactions.[17] To explicitly illustrate this generalization, we have also aligned the canonical protein−ligand assay—biotin binding to streptavidin—when using a longer PEG linker, as is common in such assays (Figure S4).[49]

CONCLUSIONS

We have developed an efficient algorithm to correct for geometric errors in AFM-based SMFS. Our three-step algorithm was comparatively fast (15−25 s), performed at low force (10−20 pN), and implemented on an unmodified commercial AFM. For DNA-based assays, we not only improved accuracy and precision but also did so with improved throughput, acquiring 88 geometrically corrected force-extension curves in ~40 min. Such high throughput, in turn, allowed us to characterize the distributions in lateral offsets DNA-, polyprotein-, and PEG-based assays. These results provide important experimental data that quantify the impact of uncorrected pulling geometries. In particular, the mean lateral offset for DNA-based assay was large, ~$1/4L_0$ for the two lengths of DNA measured (100 and 650 nm). Hence, achieving a vertical pulling geometry is critical to accurate AFM-based SMFS using double-stranded nucleic acids given their substantial persistence length (50 nm). More generally, our present work highlights how implementing more sophisticated data-acquisition protocols on a commercial AFM improves data quality and quantity.

METHODS

DNA Preparation. To achieve site-specific attachment, we prepared labeled DNA *via* PCR. The forward primers for the two lengths of DNA (100 and 650 nm) were terminally labeled with DBCO. The reverse primer contained four biotins. These primers were used to amplify the DNA using KOD Hot Start DNA polymerase (Novagen). The template for these PCR reactions was M13mp18 (New England BioLabs), and all DNA primers (Table S2) were purchased from Integrated DNA Technologies. The resulting PCR product was then subjected to a series of purification steps: (i) QiaQuick PCR purification kit (Qiagen); (ii) gel purification using a 1% agarose gel with the desired band excised with a razor blade followed by DNA extraction using a Freeze 'N Squeeze DNA gel extraction spin column (Bio-Rad) and concentration using an Amicon Ultra 0.5 mL 10K centrifugal Filter (Millipore); and (iii) a final QiaQuick PCR purification to remove residual agarose. The highly purified DNA product was eluted in TE [10 mM Tris-HCl (pH 8.0) 1 mM EDTA] and stored at 4 °C.

DOI: 10.1021/acsnano.7b05721
ACS Nano 2018, 12, 198−207

Polyprotein Labeling. We used a polyprotein terminally labeled at each end with a cysteine. The detailed protocol for purification was recently published.[12] To achieve a polyprotein terminally labeled with DBCO at one end and biotin at the other end, we incubated purified polyprotein (~50 μM) with 10 molar equiv of maleimide-DBCO (Click Chemistry Tools) for 30 min at 37 °C before adding 10 molar equiv of maleimide-PEG2-biotin (ThermoFisher). Labeling was done in labeling buffer {25 mM sodium monophosphate (pH 7.1), 150 mM NaCl, and 1 mM TCEP [tris(2-carboxyethyl)phosphine]}. The labeling reaction continued in the dark overnight at 37 °C. We removed the excess label using a size-exclusion column (Superdex 75 10/300 GL, GE Healthcare) equilibrated with labeling buffer. Peak fractions were pooled and concentrated using a 10 000 Da MWCO centrifugal concentrator (Amicon) to a final protein concentration of 0.5−2 mg/mL. In this scheme, only half of the polyproteins, at best, will be labeled with both DBCO and biotin, but only such heterobifunctionally labeled polyproteins were efficiently stretched between an azide-functionalized surface and a streptavidin-labeled tip (see below).

AFM Assay Preparation. Details of our surface functionalization protocol have been published.[12] Briefly, we initially cleaned the glass coverslips in concentrated KOH, rinsed with ultrapure water, and dried using dry nitrogen gas. We then exposed the coverslips to UV-ozone radiation (BondWand, Electro-Lite Corp.) for 1 h and then immersed them in a solution of 0.15 mg/mL silane-PEG$_{MW=600}$-azide (PG2-AZSL-600, Nanocs Inc.) dissolved in toluene at 60 °C for 3 h. Coverslips were then rinsed in toluene, isopropyl alcohol, and ultrapure water. We then rapidly dried the coverslips using dry nitrogen gas. We placed a 20 μL drop of DBCO-labeled biomolecules (5−40 ng/μL DNA or 50 ng/μL protein) onto the azide-PEG-coated coverslip and incubated them overnight at 4 °C. Varying the deposition concentration was used to coarsely tune the yield of attachments to single molecules and the ratio of single attachments to multiple attachments. Although the surface concentration was not optimized for achieving the highest yield of single attachments in the present work, we note that this protocol has achieved yields for high-quality force-extension curves resulting from stretching single molecules of 15% for the polyprotein-based assay and 19% for 650 nm DNA when scanning the surface in a raster-based pattern.[12] Finally, we rinsed the coverslips with PBS [10 mM phosphate buffer (pH 7.4), 140 mM NaCl, 3 mM KCl] buffer to remove any unbound molecules and stored them in buffer at 4 °C until use.

To improve force stability, we removed the gold and underlying chrome from BioLever Long cantilevers [L = 100 μm; k = 7 pN/nm (nominal), Olympus], providing sub-piconewton stability over 100 s.[9] Prior to functionalization, we then cleaned the AFM tips with toluene, ethanol, and water. Next, we exposed the AFM tips to UV ozone radiation for 1 h and then immersed them in a solution of 0.15 mg/mL silane-PEG$_{MW=600}$-maleimide (PG2-MLSL-600, Nanocs Inc.) dissolved in toluene at 60 °C for 3 h. AFM tips were rinsed in toluene, isopropyl alcohol, and ultrapure water. We then immersed the AFM tips in a saturating concentration of thiol-labeled streptavidin [0.2 mg/mL (SAVT, Protein Mods LLC)] for 3 h in PBS (pH 6.75). The streptavidin-coated AFM tips were then rinsed in three serial washes of PBS (pH 7.4) and stored in PBS (pH 7.4) at 4 °C prior to and between use. Finally, to demonstrate geometric alignment of a PEG-based protein−ligand assay, we used a longer PEG construct. Specifically, we functionalized the surface with a 100:1 mixture of silane-PEG$_{MW=10k}$-methoxy (PG1-SL-10k, Nanocs Inc.) relative to silane-PEG$_{MW=10k}$-biotin (PG2-BNSL-10k, Nanocs Inc.) in conjunction with our streptavidin-labeled tips prepared as described above.

AFM Experiments. All experiments were performed on a Cypher ES AFM (Asylum Research) in PBS (pH 7.4). The sample temperature was held constant at 25 °C using a temperature-controlled, closed-fluidic liquid chamber. We determined each cantilever's stiffness using the standard thermal method.[50] After calibration, the larger data-acquisition protocol (Figure S1) probed the surfaces at various locations to find molecules tethered to the surface. Within one cycle, the algorithm brought the tip toward the surface at constant velocity (v = 1000 nm/s for DNA, 500 nm/s for NuG2) until a user-defined force was achieved, typically 100 pN. To promote site-specific attachment at this comparatively low force, the tip was held in contact at constant F for 2 s. Next, the tip was retracted at constant velocity (1000 nm/s for DNA, 600 nm/s for NuG2). If a molecule of interest was attached, which is defined as reaching a preset force at a minimal extension change, the algorithm stopped retraction. After such triggering, the rest of the alignment algorithm was executed, as outlined in Figure 2. Finally, after this alignment, the tip was brought into gentle contact with the surface (F = 100 pN), and we then acquired an aligned force-extension curve by retracting the tip at constant velocity (1000 nm/s for DNA, 400 nm/s for NuG2) while digitizing at 50 kHz or 5 MHz, depending on the application.

ASSOCIATED CONTENT

Supporting Information

The Supporting Information is available free of charge on the ACS Publications website at DOI: 10.1021/acsnano.7b05721.

Diagram illustrating the logic of the data-acquisition algorithm, force-extension traces showing DNA over-stretching at several various z_{offset} and an overlay of aligned *versus* unaligned traces, histogram of r_{offset} of a PEG linker based assay, and tables listing PCR primers' sequence and algorithm parameters for different substrates (PDF)

AUTHOR INFORMATION

Corresponding Author

*E-mail: tperkins@jila.colorado.edu.

ORCID

Thomas T. Perkins: 0000-0003-4826-9490

Notes

The authors declare no competing financial interest.

ACKNOWLEDGMENTS

We thank J. Bemis and J. Cleveland for technical discussions, M.-A. LeBlanc and M. Sousa for generously providing labeled polyprotein, and L. Uyetake for DNA preparation. R.W. was supported by a fellowship from the National Research Council. This work was supported by the National Science Foundation (DBI-1353987; Phy-1734006) and NIST. Mention of commercial products is for information only; it does not imply NIST's recommendation or endorsement. T.T.P. is a staff member of NIST's Quantum Physics Division.

REFERENCES

(1) Rief, M.; Gautel, M.; Oesterhelt, F.; Fernandez, J. M.; Gaub, H. E. Reversible Unfolding of Individual Titin Immunoglobulin Domains by AFM. *Science* **1997**, *276*, 1109−1112.

(2) Florin, E.-L.; Moy, V. T.; Gaub, H. E. Adhesion Forces between Individual Ligand-Receptor Pairs. *Science* **1994**, *264*, 415−417.

(3) Moy, V. T.; Florin, E. L.; Gaub, H. E. Intermolecular Forces and Energies between Ligands and Receptors. *Science* **1994**, *266*, 257−259.

(4) Lee, G. U.; Chrisey, L. A.; Colton, R. J. Direct Measurement of the Forces between Complementary Strands of DNA. *Science* **1994**, *266*, 771−773.

(5) Clausen-Schaumann, H.; Rief, M.; Tolksdorf, C.; Gaub, H. E. Mechanical Stability of Single DNA Molecules. *Biophys. J.* **2000**, *78*, 1997−2007.

(6) Bustamante, C.; Bryant, Z.; Smith, S. B. Ten Years of Tension: Single-Molecule DNA Mechanics. *Nature* **2003**, *421*, 423−427.

(7) Greenleaf, W. J.; Woodside, M. T.; Block, S. M. High-Resolution, Single-Molecule Measurements of Biomolecular Motion. *Annu. Rev. Biophys. Biomol. Struct.* **2007**, *36*, 171−190.

(8) Neuman, K. C.; Nagy, A. Single-Molecule Force Spectroscopy: Optical Tweezers, Magnetic Tweezers and Atomic Force Microscopy. *Nat. Methods* **2008**, *5*, 491−505.
(9) Churnside, A. B.; Sullan, R. M.; Nguyen, D. M.; Case, S. O.; Bull, M. S.; King, G. M.; Perkins, T. T. Routine and Timely Sub-picoNewton Force Stability and Precision for Biological Applications of Atomic Force Microscopy. *Nano Lett.* **2012**, *12*, 3557−3561.
(10) Bull, M. S.; Sullan, R. M.; Li, H.; Perkins, T. T. Improved Single Molecule Force Spectroscopy Using Micromachined Cantilevers. *ACS Nano* **2014**, *8*, 4984−4995.
(11) Yu, H.; Siewny, M. G.; Edwards, D. T.; Sanders, A. W.; Perkins, T. T. Hidden Dynamics in the Unfolding of Individual Bacteriorhodopsin Proteins. *Science* **2017**, *355*, 945−950.
(12) Walder, R.; LeBlanc, M.-A.; Van Patten, W. J.; Edwards, D. T.; Greenberg, J. A.; Adhikari, A.; Okoniewski, S. R.; Sullan, R. M. A.; Rabuka, D.; Sousa, M. C.; Perkins, T. T. Rapid Characterization of a Mechanically Labile α-Helical Protein Enabled by Efficient Site-Specific Bioconjugation. *J. Am. Chem. Soc.* **2017**, *139*, 9867−9875.
(13) Perkins, T. T. Angstrom-Precision Optical Traps and Applications. *Annu. Rev. Biophys.* **2014**, *43*, 279−302.
(14) Hagerman, P. J. Flexibility of DNA. *Annu. Rev. Biophys. Biophys. Chem.* **1988**, *17*, 265−286.
(15) Kienberger, F.; Pastushenko, V. P.; Kada, G.; Gruber, H. J.; Riener, C.; Schindler, H.; Hinterdorfer, P. Static and Dynamical Properties of Single Poly(Ethylene Glycol) Molecules Investigated by Force Spectroscopy. *Single Mol.* **2000**, *1*, 123−128.
(16) Kulic, I. M.; Mohrbach, H.; Lobaskin, V.; Thaokar, R.; Schiessel, H. Apparent Persistence Length Renormalization of Bent DNA. *Phys. Rev. E* **2005**, *72*, 041905.
(17) Farrance, O. E.; Paci, E.; Radford, S. E.; Brockwell, D. J. Extraction of Accurate Biomolecular Parameters from Single-Molecule Force Spectroscopy Experiments. *ACS Nano* **2015**, *9*, 1315−1324.
(18) Hoffmann, T.; Dougan, L. Single Molecule Force Spectroscopy Using Polyproteins. *Chem. Soc. Rev.* **2012**, *41*, 4781−4796.
(19) Ke, C.; Jiang, Y.; Rivera, M.; Clark, R. L.; Marszalek, P. E. Pulling Geometry-Induced Errors in Single Molecule Force Spectroscopy Measurements. *Biophys. J.* **2007**, *92*, L76−78.
(20) Lee, Y.; Kwon, S. H.; Kim, Y.; Lee, J. B.; Park, J. W. Mapping of Surface-Immobilized DNA with Force-Based Atomic Force Microscopy. *Anal. Chem.* **2013**, *85*, 4045−4050.
(21) Cluzel, P.; Lebrun, A.; Heller, C.; Lavery, R.; Viovy, J. L.; Chatenay, D.; Caron, F. DNA: An Extensible Molecule. *Science* **1996**, *271*, 792−794.
(22) Smith, S. B.; Cui, Y.; Bustamante, C. Overstretching of B-DNA: The Elastic Response of Individual Double-Stranded and Single Stranded DNA Molecules. *Science* **1996**, *271*, 795−799.
(23) Kuhner, F.; Erdmann, M.; Gaub, H. E. Scaling Exponent and Kuhn Length of Pinned Polymers by Single Molecule Force Spectroscopy. *Phys. Rev. Lett.* **2006**, *97*, 218301.
(24) Rivera, M.; Lee, W.; Ke, C.; Marszalek, P. E.; Cole, D. G.; Clark, R. L. Minimizing Pulling Geometry Errors in Atomic Force Microscope Single Molecule Force Spectroscopy. *Biophys. J.* **2008**, *95*, 3991−3998.
(25) Rickgauer, J. P.; Fuller, D. N.; Smith, D. E. DNA as a Metrology Standard for Length and Force Measurements with Optical Tweezers. *Biophys. J.* **2006**, *91*, 4253−4257.
(26) Liphardt, J.; Onoa, B.; Smith, S. B.; Tinoco, I. J.; Bustamante, C. Reversible Unfolding of Single RNA Molecules by Mechanical Force. *Science* **2001**, *292*, 733−737.
(27) Woodside, M. T.; Behnke-Parks, W. M.; Larizadeh, K.; Travers, K.; Herschlag, D.; Block, S. M. Nanomechanical Measurements of the Sequence-Dependent Folding Landscapes of Single Nucleic Acid Hairpins. *Proc. Natl. Acad. Sci. U. S. A.* **2006**, *103*, 6190−6195.
(28) Bornschlogl, T.; Rief, M. Single-Molecule Protein Unfolding and Refolding Using Atomic Force Microscopy. *Methods Mol. Biol.* **2011**, *783*, 233−250.
(29) Edwards, D. T.; Faulk, J. K.; Sanders, A. W.; Bull, M. S.; Walder, R.; LeBlanc, M. A.; Sousa, M. C.; Perkins, T. T. Optimizing 1-μs-Resolution Single-Molecule Force Spectroscopy on a Commercial Atomic Force Microscope. *Nano Lett.* **2015**, *15*, 7091−7098.
(30) Edwards, D. T.; Faulk, J. K.; LeBlanc, M. A.; Perkins, T. T. Force Spectroscopy with 9-μs Resolution and Sub-pN Stability by Tailoring AFM Cantilever Geometry. *Biophys. J.* **2017**, *113*, 2595−2600.
(31) Popa, I.; Berkovich, R.; Alegre-Cebollada, J.; Badilla, C. L.; Rivas-Pardo, J. A.; Taniguchi, Y.; Kawakami, M.; Fernandez, J. M. Nanomechanics of Halotag Tethers. *J. Am. Chem. Soc.* **2013**, *135*, 12762−12771.
(32) Schoeler, C.; Malinowska, K. H.; Bernardi, R. C.; Milles, L. F.; Jobst, M. A.; Durner, E.; Ott, W.; Fried, D. B.; Bayer, E. A.; Schulten, K.; Gaub, H. E.; Nash, M. A. Ultrastable Cellulosome-Adhesion Complex Tightens under Load. *Nat. Commun.* **2014**, *5*, 5635.
(33) Fukuma, T.; Jarvis, S. P. Development of Liquid-Environment Frequency Modulation Atomic Force Microscope with Low Noise Deflection Sensor for Cantilevers of Various Dimensions. *Rev. Sci. Instrum.* **2006**, *77*, 043701.
(34) Meier, T.; Forste, A.; Tavassolizadeh, A.; Rott, K.; Meyners, D.; Groger, R.; Reiss, G.; Quandt, E.; Schimmel, T.; Holscher, H. A Scanning Probe Microscope for Magnetoresistive Cantilevers Utilizing a Nested Scanner Design for Large-Area Scans. *Beilstein J. Nanotechnol.* **2015**, *6*, 451−461.
(35) Miyazawa, K.; Kobayashi, N.; Watkins, M.; Shluger, A. L.; Amano, K.; Fukuma, T. A Relationship between Three-Dimensional Surface Hydration Structures and Force Distribution Measured by Atomic Force Microscopy. *Nanoscale* **2016**, *8*, 7334−7342.
(36) Walder, R. *Centering Github Repository*; https://github.com/robwalder/Centering (accessed July 8, 2017).
(37) Wang, M. D.; Yin, H.; Landick, R.; Gelles, J.; Block, S. M. Stretching DNA with Optical Tweezers. *Biophys. J.* **1997**, *72*, 1335−1346.
(38) Wenner, J. R.; Williams, M. C.; Rouzina, I.; Bloomfield, V. A. Salt Dependence of the Elasticity and Overstretching Transition of Single DNA Molecules. *Biophys. J.* **2002**, *82*, 3160−3169.
(39) Williams, M. C.; Wenner, J. R.; Rouzina, I.; Bloomfield, V. A. Entropy and Heat Capacity of DNA Melting from Temperature Dependence of Single Molecule Stretching. *Biophys. J.* **2001**, *80*, 1932−1939.
(40) Zhang, X.; Chen, H.; Fu, H.; Doyle, P. S.; Yan, J. Two Distinct Overstretched DNA Structures Revealed by Single-Molecule Thermodynamics Measurements. *Proc. Natl. Acad. Sci. U. S. A.* **2012**, *109*, 8103−8108.
(41) Paik, D. H.; Perkins, T. T. Overstretching DNA at 65 pN Does Not Require Peeling from Free Ends or Nicks. *J. Am. Chem. Soc.* **2011**, *133*, 3219−3221.
(42) te Riet, J.; Katan, A. J.; Rankl, C.; Stahl, S. W.; van Buul, A. M.; Phang, I. Y.; Gomez-Casado, A.; Schon, P.; Gerritsen, J. W.; Cambi, A.; Rowan, A. E.; Vancso, G. J.; Jonkheijm, P.; Huskens, J.; Oosterkamp, T. H.; Gaub, H.; Hinterdorfer, P.; Figdor, C. G.; Speller, S. Interlaboratory Round Robin on Cantilever Calibration for AFM Force Spectroscopy. *Ultramicroscopy* **2011**, *111*, 1659−1669.
(43) Edwards, D. T.; Perkins, T. T. Optimizing Force Spectroscopy by Modifying Commercial Cantilevers: Improved Stability, Precision, and Temporal Resolution. *J. Struct. Biol.* **2017**, *197*, 13−25.
(44) Carrion-Vazquez, M.; Oberhauser, A. F.; Fowler, S. B.; Marszalek, P. E.; Broedel, S. E.; Clarke, J.; Fernandez, J. M. Mechanical and Chemical Unfolding of a Single Protein: A Comparison. *Proc. Natl. Acad. Sci. U. S. A.* **1999**, *96*, 3694−3699.
(45) Ott, W.; Jobst, M. A.; Schoeler, C.; Gaub, H. E.; Nash, M. A. Single-Molecule Force Spectroscopy on Polyproteins and Receptor-Ligand Complexes: The Current Toolbox. *J. Struct. Biol.* **2017**, *197*, 3−12.
(46) Carrion-Vazquez, M.; Marszalek, P. E.; Oberhauser, A. F.; Fernandez, J. M. Atomic Force Microscopy Captures Length Phenotypes in Single Proteins. *Proc. Natl. Acad. Sci. U. S. A.* **1999**, *96*, 11288−11292.

DOI: 10.1021/acsnano.7b05721
ACS Nano 2018, 12, 198−207

(47) Cao, Y.; Balamurali, M. M.; Sharma, D.; Li, H. B. A Functional Single-Molecule Binding Assay *Via* Force Spectroscopy. *Proc. Natl. Acad. Sci. U. S. A.* **2007**, *104*, 15677−15681.
(48) He, C.; Hu, C.; Hu, X.; Hu, X.; Xiao, A.; Perkins, T. T.; Li, H. Direct Observation of the Reversible Two-State Unfolding and Refolding of an α/β Protein by Single-Molecule Atomic Force Microscopy. *Angew. Chem., Int. Ed.* **2015**, *54*, 9921−9925.
(49) Hinterdorfer, P.; Dufrene, Y. F. Detection and Localization of Single Molecular Recognition Events Using Atomic Force Microscopy. *Nat. Methods* **2006**, *3*, 347−355.
(50) Proksch, R.; Schaffer, T. E.; Cleveland, J. P.; Callahan, R. C.; Viani, M. B. Finite Optical Spot Size and Position Corrections in Thermal Spring Constant Calibration. *Nanotechnology* **2004**, *15*, 1344−1350.

DOI: 10.1021/acsnano.7b05721
ACS Nano 2018, 12, 198−207